DOI: 10.71762/5m06-ps04

Research Paper

An Improved Analytical Model for Prediction of Residual Deformation in Longitudinal Scheme of Laser Tube Forming Process

Hossein Ebrahimi[1*], Zohreh Ebrahimi[2]

[1]Department of Materials Science and Engineering, Sharif University of Technology, Azadi Ave., Tehran, Iran

[2]Mechanical Engineering Department, Payame Noor University (PNU), P.O.Box 19395-4697 Tehran, Iran

[*]Email of the Corresponding Author: z.ebrahimi@pnu.ac.ir

Received: August 23, 2024; Accepted: November 5, 2024

Abstract

Laser tube bending is a new procedure for bending tubes in industrial applications. Laser scanning can be performed using circumferential and longitudinal schemes. In this paper, an analytical model was developed to predict the effects of the longitudinal scanning scheme on the laser forming of tubes. Moreover, the effects of laser parameters and tube dimensions on residual deformation are investigated for the longitudinal scanning scheme. The presented analytical model can be utilized as a powerful tool to determine the residual bending angle, residual strain, and curvatures. To apply the proposed analytical model, a hollow tube made of mild steel is considered. The residual strain and curvature were evaluated after one pass of laser scanning for the longitudinal scheme. The results revealed that increasing the laser beam diameter leads to a reduction in the residual deformation of the tube. Furthermore, the residual tube deformation was enhanced by increasing the laser power or decreasing the laser scanning velocity.

Keywords

Laser Tube Forming, Axial Scanning Scheme, Bending Angle, Residual Deformation, Analytical Model

1. Introduction

The papers Laser forming process has been considered a new and suitable technique for manufacturing and bending mechanical parts, without external forces during the last two decades. It allows automation of manufacturing processes in the aerospace, automobile, and shipbuilding industries [1-3]. The technique offers various engineering advantages compared to common forming processes. The known advantages consist of design flexibility, the manufacture of complex shapes, and the possibility of rapid prototyping [4-5]. In this process, external forces and dies are unnecessary, and various shapes can be produced [6].

Parts in the shape of the tube are used as gas/liquid pipes in automobiles, heat exchangers, hydraulic systems, and boilers [7]. For these applications, the tubes should be bent. Instead of mechanical

bending techniques, metal forming processes can be used to reduce production steps and waste of raw material and to increase manufacturing speed [8-9].

A laser forming process can be utilized to apply a temperature field due to heat imposed on the tube. Laser bending of tubes has several advantages over mechanical bending techniques. In laser tube forming, hard bending tools and external forces are not required; hence, in the case of small-batch production and prototyping, the final cost of the product is reduced. Smaller ovalization would occur in the laser tube forming process and the tube wall thickness reduction is avoided. The laser tube bending process can be automated using numerical control systems. When some materials are bent mechanically, to prevent fracture, after each pass of bending, an annealing process should be performed. Bending of the tubes made from such materials can be performed by the laser forming process, without multiple annealing. Tubes with various cross-sectional shapes, such as circular and square, can be bent using the laser forming process. However, most of the recent efforts have been conducted in the case of tubes with circular cross-sections [7]. The laser forming of the tubes with circular cross-sections is considered in this study since tubes with circular cross-sections have vast industrial applications.

The laser tube forming can be carried out by two different kinds of laser scanning schemes, namely circumferential and longitudinal (axial) schemes. A schematic of these schemes is illustrated in Figure 1. In the circumferential scheme, the laser beam is scanned along the tube's circumference through a prescribed scanning angle up to 180°. The subsequent laser scans can be performed at the same longitudinal location with fully overlapping multiple scans along the same path or at different longitudinal locations with separate multiple scans. The tube bending can also be achieved by a laser beam scanning along the axial direction of the tube. The longitudinal scanning scheme results in a higher bending angle compared with the circumferential scanning scheme.

Many efforts have been performed to study the laser tube bending by the circumferential scanning scheme but a few studies have been carried out using the axial scanning scheme. In the case of circumferential scanning, numerous experimental, analytical, and numerical analyses are found in the literature. Li and Yao [10] investigated the mechanism of the laser tube bending process by numerical and experimental procedures. Different phenomena of the deformation process such as wall thickness variation, ovalization, and bending radius were studied in their work. Hao and Li [11] proposed an analytical model to estimate the bending angle in the laser tube bending. They verified the analytical predictions with the experimental results and reported a good agreement between the two sets of results. In another research [12], they studied the mechanism of the process using the finite element method. They obtained spatial and temporal distributions of temperature, stress, and strain fields. Hsieh and Lin [13] simulated the transient state of a thin metal tube deforming by the laser buckling mechanism and applying an axial preload. They have verified the FEM results by comparing them with experimental results and showed that by using the compressive axial preload, a larger bending angle can be achieved.

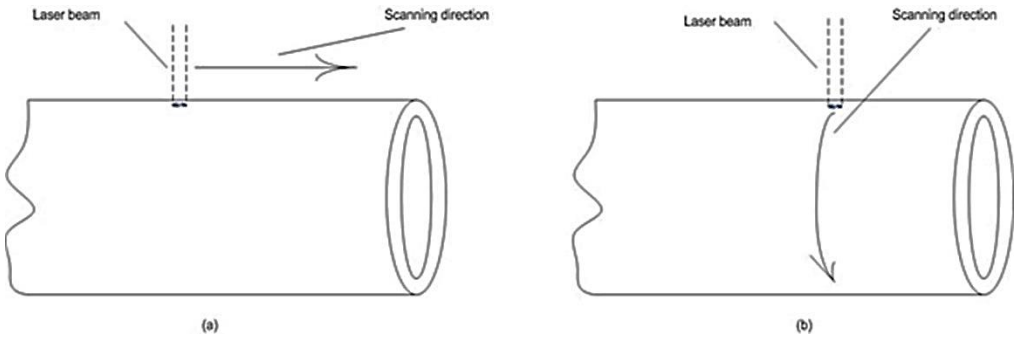

Figure 1. Schematic of the scanning schemes a) longitudinal (axial) scanning b) circumferential scanning

In the case of the axial scanning scheme, less effort has been carried out in contrast to the circumferential scheme. Zhang et al. [14] assessed the bending mechanism and characteristics of longitudinal and circumferential scanning schemes by a numerical analysis. They reported that using the axial scanning scheme, a higher bending angle compared with the circumferential scanning scheme is obtained. The scanning scheme has a significant influence on the laser forming of tube specimens. Safdar et al. [15] studied the effects of scanning schemes on bending angle in laser tube bending using a finite element model. The results revealed that the longitudinal scanning scheme results in twice the bending angle as compared to the circumferential scheme.

Parameters such as laser power, beam diameter, scan speed, specimen thickness, and heating position can significantly affect the resulting bending angle in the laser bending process. Hao and Gai [16] performed a transient thermo-mechanical analysis of a thin wall tube using the FE method. They studied the effects of laser bending parameters and concluded that the protrusion at bending intrados is more severe for thinner tubes. Zahrani, and Marasi [17] modeled the laser bending process via a response surface method and investigated the influence of model parameters on the bending angle. A thermo-mechanical FE model has been developed by Venkadeshwaran et al. [18] to simulate the laser bending process. They investigated laser power, scan velocity, and specimen thickness on the bend angle and obtained optimum parameters to increase productivity and decrease the operating cost. Guan et al. [19] simulated the single and multi-scan laser tube bending process using a thermo-mechanical FE model. The study's results revealed that the bending angle induced by the first irradiated time was largest and the relation between the number of scans and the bending angle was in direct ratio. Jamil et al. [20] presented an FE analysis of laser bending of nickel tubes. The results indicated that the tube bending angle increases by applying a constraint at the tube free-end. Li et al. [21] studied the mechanism of the laser tube bending process and the effects of process parameters, such as laser power, scanning time, and speeds, on the bending angle with both the FE method and experiments. They found that the bending angle increases with increasing the laser power and decreasing the scanning speed. Keshtiara et al. [22] studied the effects of various laser beam parameters on the tube bending process. They achieved optimum process parameters for tube bending angle with minimum ovality and wall thickening. Safari [23] experimentally investigated the effects of the irradiating length and irradiating passe number on the bending angle in laser bending of a mild steel tube. The results indicated that with an increase in the irradiating length and passes, the main bending angle increases.

Folkersma et al. [24] developed a tube laser bending process to align optical fibers to a photonic integrated. They achieved a high precision in the alignment of optical fiber. Imhan et al. [25] presented a modified analytical model of laser tube bending, by considering the effects of material specifications variation due to the temperature rise in the laser of the tubes. He et al. [26] reported that several main defects, such as springback phenomena, thinning in the tube wall, cross-section deformation, and wrinkling instabilities, which appear in traditional tube bending processes, happen rarely in the laser tube bending process. Khandandel et al. [27] analyzed the bending angle and microstructure of the tube after laser tube bending by imposing forced cooling at different distances from the laser beam. With applying local cooling, the duration of the tube bending process was reduced considerably. Safari et al. [28] have investigated the effects of process parameters on main and lateral bending angles in the laser tube bending process. They reported that the main bending angle increases by increasing the irradiation length, irradiation pass number, and laser power. The results indicate the axial scanning scheme produces a much higher bending angle than the circumferential scanning scheme for similar conditions. The effects of different laser scanning strategies on the bending angle of steel plates are investigated by Dong et al. [29]. Wang et al. [30] conducted the method of irradiating schemes for laser tube bending, which evaluates the curvatures of the tubes. They have concluded that the presented scanning path planning was feasible and effective. The circumferential scanning scheme achieves a small bending angle per scan and thus requires multiple scans to obtain practical bending angles. This process is too time-consuming. However, the advantage of the axial scanning scheme is that it generates sufficient bending in a single axial scan [14]. Hence, the axial scanning scheme results in greater angular deformation than the circumferential scanning scheme. The produced bending angle is greater in the axial scanning scheme, which would decrease the number of scans required. Therefore, the axial scanning scheme in laser tube forming is considered in the presented study.

To the best of the authors' knowledge, there is not any analytical model yet in the literature to analyze the axial scheme in the laser tube forming process. Therefore, in this work, an analytical model is developed to predict the effects of different laser parameters, such as laser scanning velocity, laser power, and laser beam diameter and dimensions of the tube, on the deformation of the tube in the axial scheme. Moreover, the proposed analytical model can predict the bending angle in terms of residual strain and curvature of the tube.

2. Materials and Methods

To inquire about the deformation of the tube, at first, the temperature distribution along the thickness direction of the tube should be known. According to Shen et al. [4], the temperature change along the thickness direction can be expressed as Equation (1),

$$\Delta T = \frac{2PA}{\rho\, C\, u\, h\, d} \exp\left(-\frac{\rho\, C\, u}{2\, k}\left(z + \frac{h}{2}\right)\right) \quad (1)$$

Where z is the distance from the middle of the tube thickness, ΔT the temperature change, P is the laser power, A the absorption coefficient of the material, u is the laser scanning velocity, h is the tube thickness, d is the laser beam diameter, and ρ, C, and k are the density, specific heat, and thermal

conductivity of the tube material, respectively. By taking the integration from both sides of Equation (1), the average temperature change in the z direction is obtained as Equation (2),

$$T_{up} = \frac{2PA}{\rho\, C\, u\, h^2 d}\int_{-\frac{h}{2}}^{\frac{h}{2}} \exp\left(-\frac{\rho\, C\, u}{2\, k}\left(z+\frac{h}{2}\right)\right) dz = \frac{4PA\, k\left(1-\exp\left(-\frac{\rho\, C\, u\, h}{2\, k}\right)\right.}{\rho^2 C^2 u^2 h^2 d} \quad (2)$$

Where T_{up} is the average temperature change due to laser irradiation. The half angle of the irradiated tube material in the hoop direction (Φ), which is illustrated in Figure 2, can be expressed as Equation (3) [28].

$$\Phi = \arcsin\left(\frac{d}{2b}\right) \quad (3)$$

To develop the analytical model, the following assumptions were made:
(1) Any plane normal to the neutral axis remains plane during the bending.
(2) The material properties are independent of temperature and direction.
(3) The temperature distribution of the tube does not change with time. So, the heat conduction in the specimen, thermal radiation to the air, and free convection are balanced and temperature distribution is not affected by them.
(4) The laser intensity distribution is uniform.
(5) The heat generation due to the strain energy is negligible.
(6) Any phase change and its effects are neglected.
(7) The behavior of the tube material in tension and compression is the same.
(8) The tube material is incompressible in the plastic deformation range.
(9) The tube material is elastic-perfectly plastic.
(10) Any normal and shear stress, except the axial stress, is negligible. So the state of stress is one-dimensional.

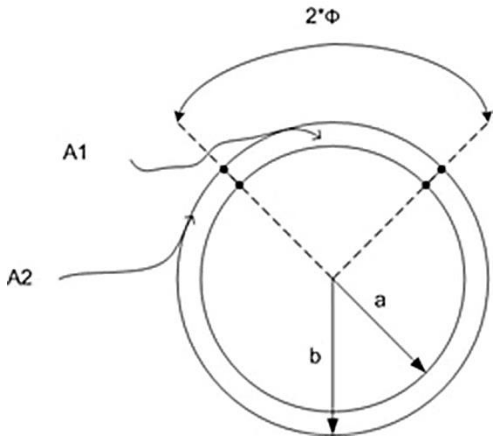

Figure 2. Schematic of the cross-section of the tube

Regarding the last assumption, the elastic strain energy per unit volume, Π, can be expressed as Equation (4),

$$\Pi = \frac{1}{2}\int_V \overline{\sigma}\overline{\varepsilon}^{e}\, dV = \frac{1}{2}\int_V \overline{\sigma}_x \overline{\varepsilon}_x{}^{e}\, dV = \frac{1}{2}\int_V E\overline{\varepsilon}_x{}^{e}\, \overline{\varepsilon}_x{}^{e} dV \quad (4)$$

Where

$$\overline{\varepsilon}_x{}^{e} = \overline{\varepsilon}_x - \overline{\varepsilon}_x{}^{th} \quad (5)$$

In Equation (4) and Equation (5) $\overline{\varepsilon}_x$,$\overline{\varepsilon}_x{}^{th}$,$\overline{\varepsilon}_x{}^{e}$, E and $\overline{\sigma}_x$are the total strain, the thermal strain, the elastic strain, the young modulus, and the stress component in axial direction, respectively. According to the first assumption, the total strain component can be expressed as Equation (6).

$$\overline{\varepsilon}_x = \varepsilon_x + z\, k_x \quad (6)$$

The strain ε_x and curvature k_x of the neutral axis are given in Equation (7) and Equation (8), respectively.

$$\varepsilon_x = \frac{\partial u}{\partial x} + \frac{1}{2}\left(\frac{\partial w}{\partial x}\right)^2 \quad (7)$$

$$k_x = -\frac{\partial}{\partial x}\left(\frac{\partial w}{\partial x}\right) \quad (8)$$

In Equation (6) to Equation (8), w and u are the lateral and axial displacement components, respectively. To maintain the equilibrium, the first variation of the strain energy per unit volume should be zero. By putting the first variation equal to zero, one can get,

$$k_x = \int_{A_t} \frac{\left(\overline{\varepsilon}_x{}^{th} z\right)}{I_t}\, dA \quad (9)$$

and

$$\varepsilon_x = \int_{A_t} \frac{\overline{\varepsilon}_x{}^{th} dA}{A_t} \quad (10)$$

Where I_t and A_t are the moment of inertia and the area of the total cross-section of the tube, respectively. In the derivation of Equation (9) and Equation (10), the coordinate system was located at the centroid of the cross-section, according to Equation (11).

$$\int_{A_t} z\, dA = 0 \quad (11)$$

Replacing for k_x and ε_x from Equation (9) and Equation (10) in Equation (6) and using the Hook's law yields,

$$\bar{\sigma}_x^e = E\left\{\int_{A_t} \frac{\bar{\varepsilon}_x^{th}\, dA}{A_t} + Z\int_{A_t} \frac{(\bar{\varepsilon}_x^{th} Z)\, dA}{I_t} - \bar{\varepsilon}_x^{th}\right\} \quad (12)$$

Equation (9), Equation (10), and Equation (12) are derived based on the elastic deformation assumption. To analyze the elastic-plastic deformation in the laser tube forming, the domain where yielding takes place should be known. This domain is achieved by comparison of the absolute value of axial stress achieved from Equation (12) with the yield stress of the material. The cross-section of the tube can be divided into two areas; laser affected area (A_1) and none affected area (A_2). So the thermal strain can be defined as Equation (13),

$$\bar{\varepsilon}_x^{th} = \begin{Bmatrix} \alpha T_{up} & \text{in } A_1 \\ 0 & \text{in } A_2 \end{Bmatrix} \quad (13)$$

Where α is the thermal expansion coefficient of the tube material. Taking A_i, Z_i and I_i as area, first moment of area, and second moment of area of the tube, respectively, then they are defined as,

$$\begin{aligned} A_i &= \int_{A_i} dA \\ Z_i &= \int_{A_i} z\, dA \\ I_i &= \int_{A_i} z^2 dA \end{aligned} \quad (14)$$

Where the i notation is equal to 1 for the laser-affected area, equal to 2 for the none-affected area, and equal to t for the total area. Figure 2 shows A_1, A_2, and Φ for a circular tube. In this figure, a and b are the inner and the outer radius of the tube, respectively. Referring to Figure 2, and using Equation (14), one can write Equation (15).

$$\begin{aligned} &A_t = \pi\,(b^2 - a^2) \quad A_1 = \Phi\,(b^2 - a^2) \\ &A_2 = (\pi - \Phi)\,(b^2 - a^2) \quad I_t = \frac{\pi}{4}(b^4 - a^4) \\ &I_1 = \frac{(\Phi + 0.5\sin(2\Phi))}{4}(b^4 - a^4) \\ &I_2 = \frac{(\pi - \Phi - 0.5\sin(2\Phi))}{4}(b^4 - a^4) \\ &Z_t = 0 \quad Z_1 = -Z_2 = \frac{p}{3\,b}(b^3 - a^3) \end{aligned} \quad (15)$$

As the thermal strain is independent of the axial direction, C_1 and C_2 can be defined as,

$$C_1 = \int_{A_t} \frac{\bar{\varepsilon}_x^{th}}{A_t}\, dA \quad (16)$$

and

$$C_2 = \int_{A_t} \frac{(\bar{\varepsilon}_x^{th} z)}{I_t}\, dA \tag{17}$$

Where C_1 and C_2 in Equation (17) are constant. Therefore, Equation (12) can be rewritten as,

$$\bar{\sigma}_x^e = E\{C_1 + Z\, C_2 - \bar{\varepsilon}_x^{th}\} \tag{18}$$

By replacing Equation (13) with Equations (16) and (17), C1 and C2 can be derived. The relations of C1 and C2 are given in Equation (19) and Equation (20), respectively.

$$C_1 = \frac{\alpha\, T_{up} \Phi}{\pi} \tag{19}$$

and

$$C_2 = \frac{4\, \alpha\, T_{up} d\, (b^3 - a^3)}{3\, b\, \pi\, (b^4 - a^4)} \tag{20}$$

C_1 and C_2 refer to the state that the material behavior is elastic. At this stage, the material in A_1 is subjected to yielding, while A_2 is still in the elastic region as given in Equation (21).

$$\frac{Y}{E\,\alpha\left(1 - \frac{\Phi}{\pi} - \frac{4p}{3\pi}\frac{b^3-a^3}{b^4-a^4}\right)} \le T_{up} \le \frac{Y}{E\,\alpha\left(\frac{\Phi}{\pi} + \frac{4p}{3\pi}\frac{b^3-a^3}{b^4-a^4}\right)} \tag{21}$$

Combining Equation (2) and Equation (21) leads to Equation (22).

$$\begin{aligned} \frac{Y\,(\rho\, C\, u\, h)^2 p}{4E\alpha Ak\left(1 - \exp(-\frac{1}{2}\frac{\rho\, Cuh}{k})\right)\left(1 - \frac{\Phi}{\pi} - \frac{4p}{3\pi}\frac{b^3-a^3}{b^4-a^4}\right)} &\le P_r \\ \le \frac{Y\,(\rho\, C\, u\, h)^2 p}{4E\alpha Ak\left(1 - \exp(-\frac{1}{2}\frac{\rho Cuh}{k})\right)\left(\frac{\Phi}{\pi} + \frac{4p}{3\pi}\frac{b^3-a^3}{b^4-a^4}\right)} & \end{aligned} \tag{22}$$

Equation (22) indicates that by choosing the proper laser power, the situation that only material in A_1 is subjected to yielding can be employed. In this situation, the stress distribution in the tube is as Equation (23),

$$\bar{\sigma}_x^{ep} = \begin{cases} Y & \text{in } A_1 \\ E(C_3 + ZC_4) & \text{in } A_2 \end{cases} \tag{23}$$

Where C_3 and C_4 are unknown constants. In the absence of external moment and force, to maintain equilibrium, Equation (24) and Equation (25) should be satisfied.

$$\int_{A_t} \bar{\sigma}_x \, dA = 0 \tag{24}$$

and

$$\int_{A_t} \bar{\sigma}_x z \, dA = 0 \tag{25}$$

Considering that $A_t=A_1+A_2$ and substituting Equation (23) in Equation (24) and Equation (25), C_3 and C_4 constants are determined by solving Equation (26) and Equation (27),

$$C_3 = \frac{\frac{Y}{E}\left(\frac{d^2}{9b^2}(b^3-a^3)^2 + 0.25\,\Phi\,(\pi-\Phi-0.5\sin(2\Phi))(b^4-a^4)(b^2-a^2)\right)}{0.25\,(\pi-\Phi)(\pi-\Phi-0.5\sin(2\Phi))(b^4-a^4)(b^2-a^2) - \frac{d^2}{9b^2}(b^3-a^3)^2} \tag{26}$$

and

$$C_4 = \frac{\frac{Y\pi\,d}{3\,b\,E}(b^3-a^3)(b^2-a^2)}{0.25\,(\pi-\Phi)(\pi-\Phi-0.5\sin(2\Phi))(b^4-a^4)(b^2-a^2) - \frac{d^2}{9b^2}(b^3-a^3)^2} \tag{27}$$

The residual deformation of the neutral axis can be obtained using Equation (28) and Equation (29), respectively.

$$\varepsilon_x^p = C_3 - C_1 \tag{28}$$

$$k_x^p = C_4 - C_2 \tag{29}$$

where ε_x^p and k_x^p are residual strain and curvature of the neutral axis, respectively. Substituting Equation (19) and Equation (26) in Equation (28) and substituting Equation (20) and Equation (27) in Equation (29) yields to Equation (30) and Equation (31).

$$\varepsilon_x^p = \frac{\frac{Y}{E}\left(\frac{d^2}{9b^2}(b^3-a^3)^2 + 0.25\,\Phi\,(\pi-\Phi-0.5\sin(2\Phi))(b^4-a^4)(b^2-a^2)\right)}{0.25\,(\pi-\Phi)(\pi-\Phi-0.5\sin(2\Phi))(b^4-a^4)(b^2-a^2) - \frac{d^2}{9b^2}(b^3-a^3)^2} - \frac{\alpha T_{up}\Phi}{\pi} \tag{30}$$

$$k_x^p = \frac{\frac{Y\pi\,d}{3\,b\,E}(b^3-a^3)(b^2-a^2)}{0.25\,(\pi-\Phi)(\pi-\Phi-0.5\sin(2\Phi))(b^4-a^4)(b^2-a^2) - \frac{d^2}{9b^2}(b^3-a^3)^2} - \frac{4\,\alpha\,T_{up}\,d\,(b^3-a^3)}{3\,b\,\pi\,(b^4-a^4)} \tag{31}$$

The residual bending angle is calculated as Equation (32),

$$\theta^p = k_x^p\,L\,(1+\varepsilon_x^p) \tag{32}$$

where θ^p is the residual tube bending angle and L is the tube length. Using Equation (2), Equation (3), Equation (30), and Equation (31), the resultant bending and stretching deformation of the tube are determined during one pass of the laser scan.

3. Results and Discussion

To utilize the proposed analytical model, a tube made of mild steel with a Young modulus of E=200GPa, an absorption coefficient of A=0.6, a density of ρ=7860 kg/m^3, specific heat of C_{th}=481 J/kg.k, thermal conductivity of k_{th}=45 W/m.k, thermal expansion coefficient of $\alpha=11.6\times10^{-6}$ 1/K, yield stress of Y=250 MPa, internal radius of a=13.5 mm and external radius of b=15 mm is considered. The laser power and the scanning velocity were assumed as P=300 W and u=25 mm/s, respectively. Figure 3 shows the effect of laser beam diameter on the residual strain and curvature of the neutral axis of the tube. An increase in laser beam diameter leads to a decrease in the magnitude of residual deformation of the tube. As is seen by an increase in the laser beam diameter, the yielded area is increased and the spring-back force is reduced. Thus, the decline in the residual deformation may be attributed to the decrease in the spring-back force.

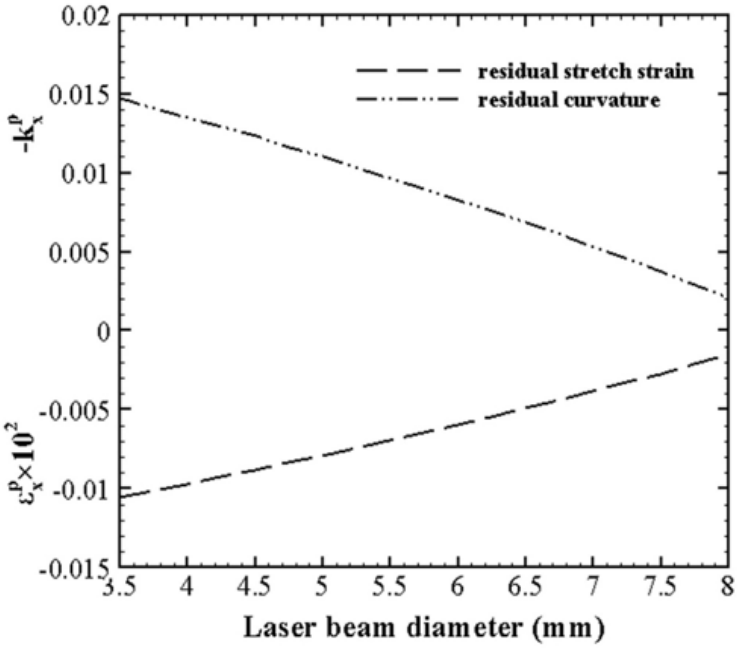

Figure 3. Effect of laser beam diameter on the residual deformation of the tube under axial scanning scheme

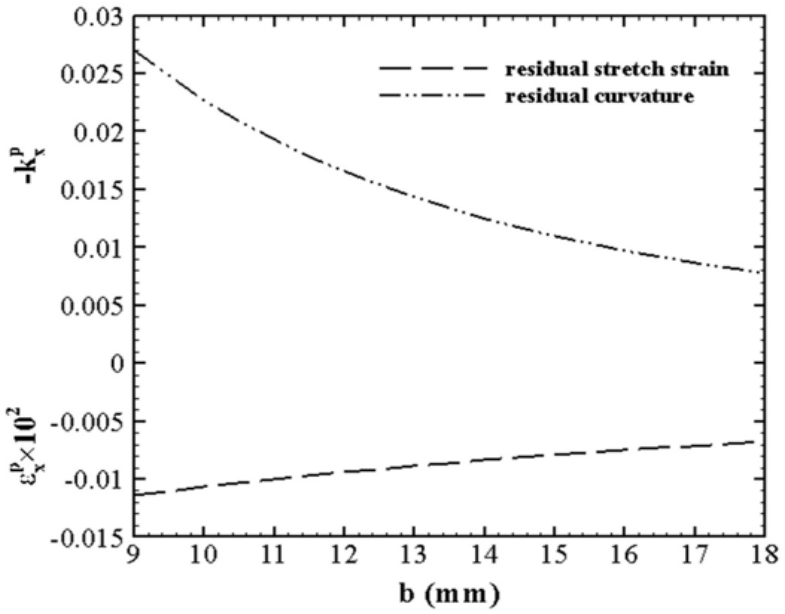

Figure 4. Effect of outer tube radius on the residual deformation of the tube under axial scanning scheme

Figure 4 exhibits the effect of the outer tube radius on the residual deformation of the tube. The laser parameters were assumed as P=300 W, u=25 mm/s, d=5 mm, and the tube thickness h=1.5 mm. The area and inertia of the cross-section increase with the enhancement of outer radius magnitude, so the resistance of the tube to the deformation is increased. Therefore, with an increase in the outer radius, the residual deformation in the tube is reduced.

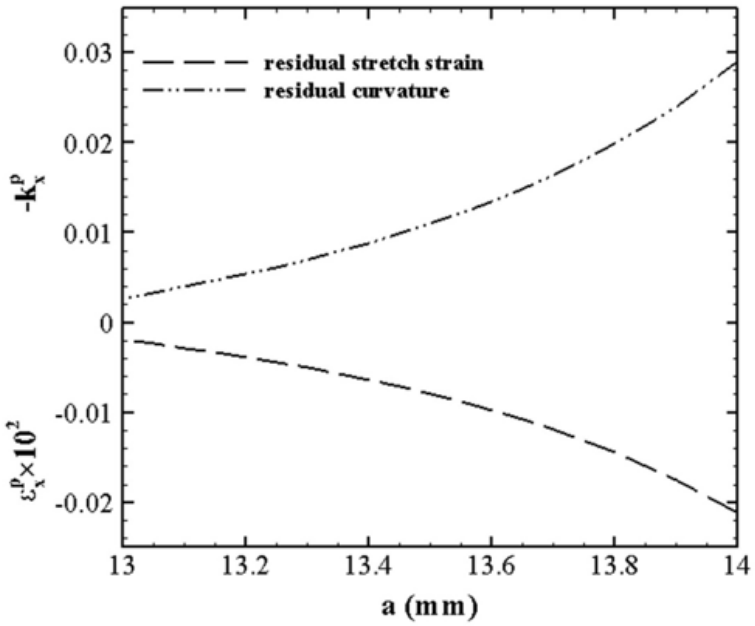

Figure 5. Effect of inner tube radius on the residual deformation of the tube under axial scanning scheme

The effect of the inner tube radius on the residual deformation, for a tube with an outer radius of b=15 mm, is depicted in Figure 5. The laser parameters are P=300 W, u=25 mm/s, and d=5 mm. As it is observed, the increase in the inner radius leads to the decline of the magnitude of the area and the

inertia of the cross-section of the tube. Hence, the resistance to the deformation is decreased and the final resultant deformation is enhanced.

Figure 6 exhibits the dependence of the residual deformation of the tube on the laser scanning velocity. The inner and outer diameter of the tube are a=13.5 mm and b=15 mm, respectively. Other laser parameters are P=300 W and d=5 mm. Referring to the figure, by increasing the scanning velocity, the lesser heat is imposed on the tube, so the resultant deformation is decreased.

Figure 7 shows the effect of the laser power on the resultant deformation of the tube. The inner and the outer diameter of the tube are a=13.5 mm and b=15 mm, respectively. The laser scanning velocity and beam diameter are supposed to be u=25 mm/s and d=5 mm, respectively. It is observed that the increase in laser power leads to the enhancement of the imposing heat and so the resultant deformation is increased.

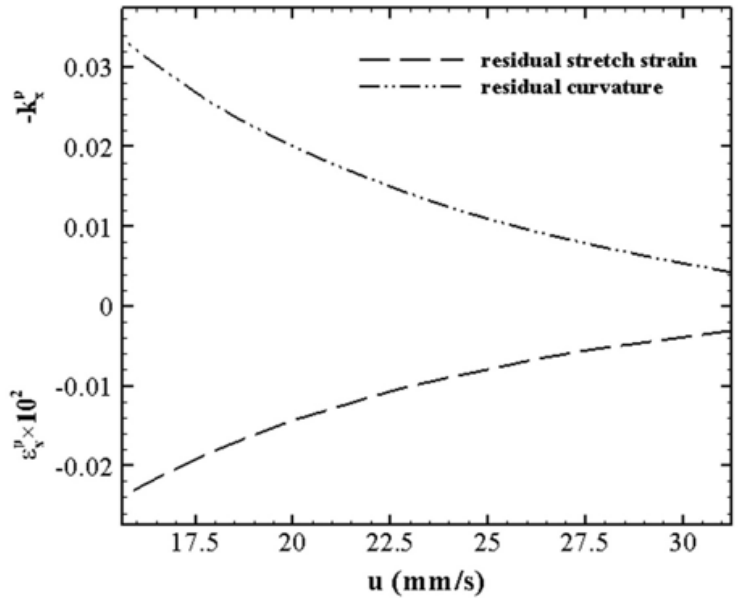

Figure 6. The effect of laser scanning velocity on the residual deformation of the tube

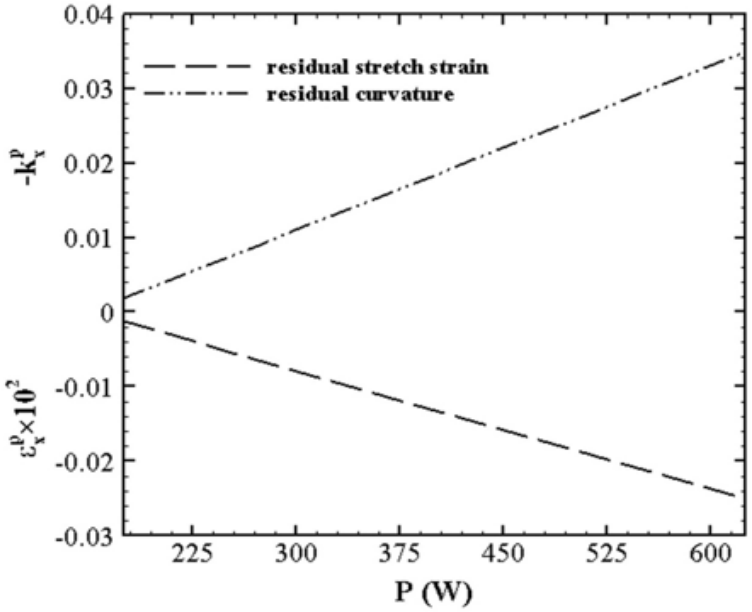

Figure 7. The effect of laser power on the residual deformation of the tube

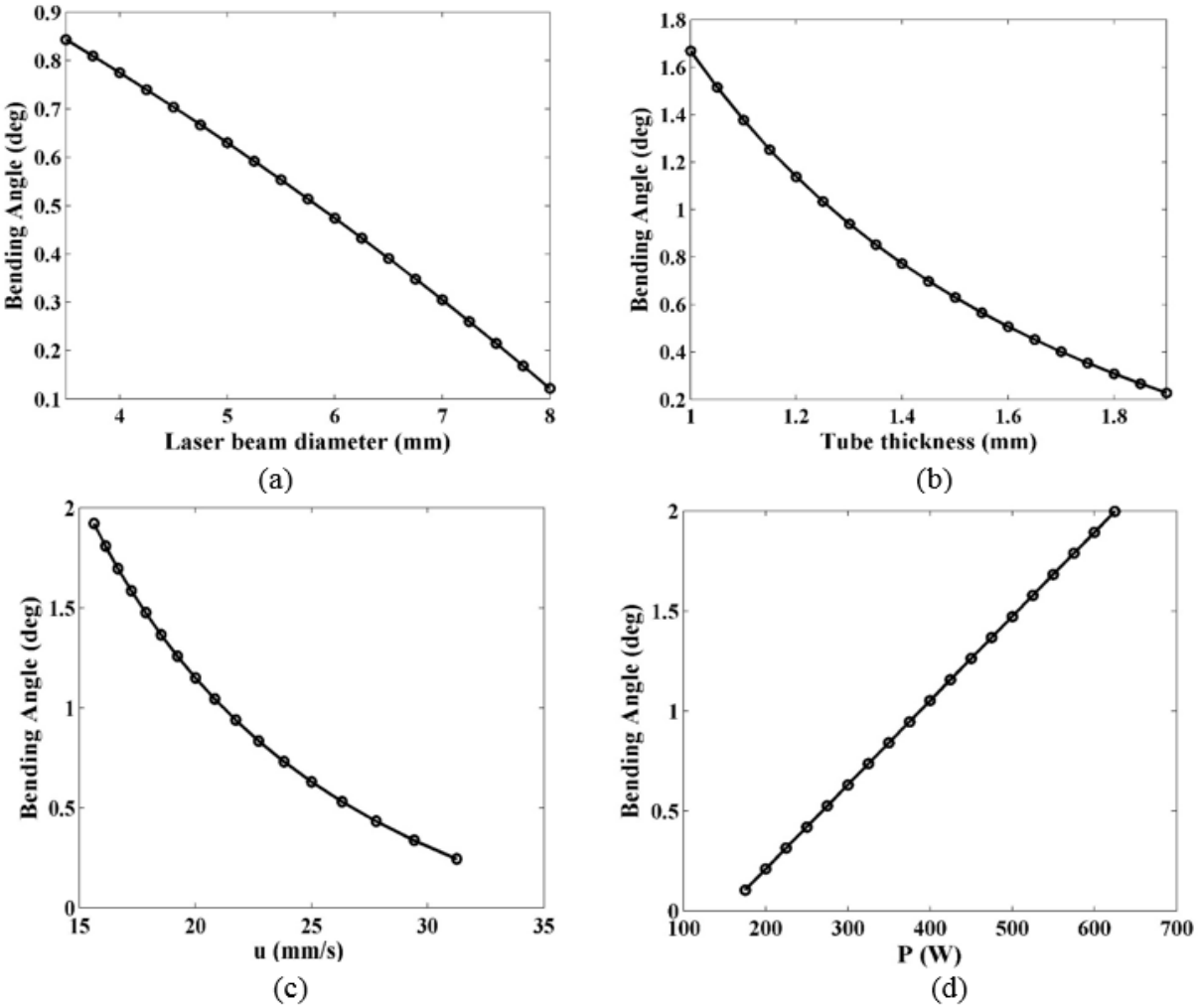

Figure 8. Evaluation of the residual tube bending angle in the axial scheme of the laser forming process; effects of a) laser beam diameter, b) tube thickness, c) laser scanning velocity, and d) laser power on the resulted bending angle

After establishing the effects of laser forming and geometrical parameters on the residual deformation of the tube, the residual bending angle can be obtained according to Equation (32). The results of the calculated bending angle are presented in Figure 8. The residual bending angle decreases with increasing laser beam diameter as shown in Figure 8(a). The laser power, scanning velocity, and tube thickness were assumed as P=300 W, u=25 mm/s, and h=1.5 mm, respectively. Other material properties are the same as in previous investigations. The decline in the residual deformation, by increasing the laser beam diameter, can be attributed to the increase of the yielded area, and hence decrease in the spring-back force.

The bending angle is decreased by increasing the tube thickness as depicted in Figure 8(b). The laser beam diameter was set to d=5 mm and other parameters are the same as in the previous investigation. The stiffness of the tube is increased by increasing the tube thickness, and hence the bending resistance of the tube is increased. Figure 8(c) indicates that by increasing the scanning velocity, the heat imposed on the tube is decreased. Therefore, the resultant deformation and the residual bending angle are decreased. Finally, the effects of laser power on residual bending angle are investigated, by setting u=25 mm/s in Figure 8(d). A linear relationship is obtained between the laser power and the

residual bending angle. In fact, by increasing the laser power, more heat is imposed on the tube. Hence, the resultant deformation and the bending angle are increased.

4. Conclusion

Laser tube bending is a new procedure for bending the tubes for the industrial applications. The laser scanning can be performed in circumferential and axial schemes. In this study, an analytical model was developed to estimate the residual deformation after one pass of scanning for the axial scheme. The following conclusions were drawn from the results:

1. By increasing in laser beam diameter, more region of the tube was subjected to yielding. Thus, the spring-back force was reduced and the residual deformation of the tube was decreased.
2. By enhancement of the tube's outer diameter with a constant thickness or by an increase in thickness for a constant outer diameter, the area and inertia of the cross-section were increased. Hence, the resistance of the tube to the deformation was enhanced. Hence the resultant deformation and the residual bending angle were decreased.
3. By an increase in laser power and/or decrease in laser scanning velocity, more heat has been imposed on the tube, hence the residual deformation of the tube was enhanced. The residual bending angle was increased consequently.

5. References

[1] Cheng, J. and Yao, Y.L. 2001. Cooling effects in multiscan laser forming. Journal of Manufacturing Processes. 3:60-72. doi: 10.1016/s1526-6125(01)70034-5.

[2] Liu, C. and Yao, Y.L. 2005. FEM-based process design for laser forming of doubly curved shapes. Journal of Manufacturing Processes. 7:109-121. doi: 10.1016/s1526-6125(05)70088-8.

[3] Cheng, P., Yao, Y.L., Liu, C., Pratt, D. and Fan, Y. 2005. Analysis and prediction of size effect on laser forming of sheet metal. Journal of Manufacturing Processes. 7:28-41. doi:10.1016/s1526-6125(05)70079-7.

[4] Shen, H., Yao, Z., Shi, Y. and Hu, J. 2006. An analytical formula for estimating the bending angle by laser forming. Proceedings of the Institution of Mechanical Engineers, Part C: Journal of Mechanical Engineering Science. 220:243-247. doi: 10.1243/095440606x79721.

[5] Shi, Y., Shen, H., Yao, Z. and Hu, J. 2007. An analytical model based on the similarity in temperature distributions in laser forming. Optics and Lasers in Engineering. 45:83-87. doi: 10.1016/j.optlaseng.2006.04.006.

[6] Aher, V. and Navthar, R.R. 2024. A Comprehensive review on laser bending of advanced materials. Lasers in Manufacturing and Materials Processing. doi: 10.1007/s40516-024-00261-w.

[7] Imhan, K.I., Baharudin, B.T.H.T, Zakaria, A., Ismail, M.I.S.B., Alsabti, N.M.H. and Ahmad, A.K. 2018. Features of laser tube bending processing based on laser forming: A Review. Journal of Lasers, Optics and Photonics. 5:174. doi: 10.4172/2469-410X.1000174.

[8] Hashemi, S.J. 2021. Investigation of the effect of different forming pressure curves on formability of AA1050 tubes in warm hydroforming process. Journal of Modern Processes in Manufacturing and Production. 10(1):52-61. dor: 20.1001.1.27170314.2021.10.1.4.3.

[9] Feizi, M. and Jafari Nedoushan, R. 2015. Finite element modeling and experimental study of the spline tube forming. Journal of Modern Processes in Manufacturing and Production. 4(2):5-12. dor: 20.1001.1.27170314.2015.4.1.4.1.

[10] Li, W. and Yao, Y.L. 2001. Laser bending of tubes: mechanism, analysis, and prediction. Journal of Manufacturing Science and Engineering. 123:674-681. doi: 10.1115/1.1392992.

[11] Hao, N. and Li, L. 2003. An analytical model for laser tube bending. Applied Surface Science. 208–209:432–436. doi: 10.1016/S0169-4332(02)01428-9.

[12] Hao, N. and Li, L. 2003. Finite element analysis of laser tube bending process. Applied Surface Science, 208:437-441. doi: 10.1016/s0169-4332(02)01429-0.

[13] Hsieh, H.S. and Lin, J. 2005. Study of the buckling mechanism in laser tube forming. Optics & Laser Technology. 37:402-409. doi: 10.1016/j.optlastec.2004.06.004.

[14] Zhang, J., Cheng, P., Zhang, W., Graham, M., Jones, J., Jones, M. and Yao, Y.L. 2006. Effects of scanning schemes on laser tube bending. Journal of Manufacturing Science and Engineering. 128:20-33. doi: 10.1115/1.2113047.

[15] Safdar, S., Li, L., Sheikh, M.A. and Liu, Z. 2007. Finite element simulation of laser tube bending: effect of scanning schemes on bending angle, distortions and stress distribution. Optics & Laser Technology. 39:1101–1110. doi: 10.1016/j.optlastec.2006.09.014.

[16] Hao, N. and Gai, Y. 2011. Numerical Simulation on the laser bending of thin wall tubes. Key Engineering Materials. 460-461:798-801. doi: 10.4028/www.scientific.net/KEM.460-461.798.

[17] Zahrani, E.G. and Marasi, A. 2012. Modeling and optimization of laser bending parameters via response surface methodology. Proc IMechE Part C: Journal of Mechanical Engineering Science. doi: 10.1177/0954406212461119.

[18] Venkadeshwaran, K., Das, S. and Misra, D. 2012. Bend angle prediction and parameter optimisation for laser bending of stainless steel using FEM and RSM. International Journal of Mechatronics and Manufacturing Systems. 5(3/4):308–321. doi: 10.1504/ijmms.2012.048237.

[19] Guan, Y., Yuan, G., Sun, S. and Zhao, G. 2013. Process simulation and optimization of laser tube bending. Int J Adv Manuf Technol. 65:333–342. doi: 10.1007/s00170-012-4172-6.

[20] Jamil, M.S.C., Fauzi, E.R.I., Juinn, C.S. and Sheikh, M.A. 2015. Laser bending of pre-stressed thin-walled nickel micro-tubes. Optics & Laser Technology. 73:105–117. doi: 10.1016/j.optlastec.2015.04.012.

[21] Li, F., Liu, S., Shi, A., Chu, Q., Shi, Q. and Li, Y. 2019. Research on laser thread form bending of stainless steel tube. International Journal of Precision Engineering and Manufacturing. 20:893–903. doi: 10.1007/s12541-019-00068-2.

[22] Keshtiara, M., Golabi, S. and Tarkesh Esfahani, R. 2019. Multi-objective optimization of stainless steel 304 tube laser forming process using GA. Engineering with Computers. 35:155-171. doi. 10.1007/s00366-019-00814-0.

[23] Safari, M. 2019. A Study on the laser tube bending process: effects of the irradiating length and the number of irradiating passes. Iranian Journal of Materials Forming. 7(1):46-53. doi: 10.22099/IJMF.2019.34213.1133.

[24] Folkersma, K.G.P., Romer, G.R.B.E., Brouwer, D.M. and Herder, J.L. 2015. High precision optical fiber alignment using tube laser bending. The International Journal of Advanced Manufacturing Technology. 86:953-961. doi: 10.1007/s00170-015-8143-6.

[25] Imhan, K.I, Hang Tuuah Baharudin, B.T., Zakaria, A. and Ahmad, A.K. 2017. Investigation of material specifications changes during laser tube bending and its influence on the modification and optimization of analytical modeling. Optics & Laser Technology. 95:151-156. doi: 10.1016/j.optlastec.2017.04.030.

[26] He, Y.; Li, H.; Zhang, Z. and Guangjun, L. 2012. Advances and trends on tube bending forming technologies. Chinese Journal of Aeronautics. 25:1–12. doi: 10.1016/S1000-9361(11)60356-7.

[27] Khandandel, S.E.; Seyedkashi, S.M.H. and Moradi, M. 2021. M. Numerical and experimental analysis of the effect of forced cooling on laser tube forming. Journal of the Brazilian Society of Mechanical Sciences and Engineering. 43:338. doi: 10.1007/s40430-021-03063-9.

[28] Safari, M., Alves de Sousa, R. and Joudaki, J. 2023. Comprehensive assessment of laser tube bending process by response surface methodology. Steel Research International. 94:2200230. doi. 10.1002/srin.202200230.

[29] Dong, W., Zhang, Y., Bao, L. and Shin, K. 2024. Effects of laser scanning strategy on bending behavior and microstructure of DP980 steel. Materials. 17:2415. doi. 10.3390/ma17102415.

[30] Wang, X.Y.;Wang, J.; Xu,W.J. and Guo, D.M. 2014. Scanning path planning for laser bending of straight tube into curve tube. Optics & Laser Technology. 56:43–51. doi. 10.1016/j.optlastec.2013.07.001.